

Effects of magnesium on phosphorus chemical states and p-type conduction behavior of phosphorus-doped ZnO films

Jichao Li, Yongfeng Li, Bin Yao, Ying Xu, Shiwang Long, Lei Liu, Zhenzhong Zhang, Ligong Zhang, Haifeng Zhao, and Dezhen Shen

Citation: [The Journal of Chemical Physics](#) **138**, 034704 (2013); doi: 10.1063/1.4775840

View online: <http://dx.doi.org/10.1063/1.4775840>

View Table of Contents: <http://scitation.aip.org/content/aip/journal/jcp/138/3?ver=pdfcov>

Published by the [AIP Publishing](#)



Re-register for Table of Content Alerts

Create a profile.



Sign up today!



Effects of magnesium on phosphorus chemical states and *p*-type conduction behavior of phosphorus-doped ZnO films

Jichao Li,^{1,2} Yongfeng Li,^{1,2} Bin Yao,^{1,2,a)} Ying Xu,² Shiwang Long,² Lei Liu,³ Zhenzhong Zhang,³ Ligong Zhang,³ Haifeng Zhao,³ and Dezhen Shen³

¹Key Laboratory of Physics and Technology for Advanced Batteries, Ministry of Education and College of Physics, Jilin University, Changchun, 130012, People's Republic of China

²State Key Laboratory of Superhard Materials and Department of Physics, Jilin University, Changchun 130023, People's Republic of China

³Key Laboratory of Excited State Processes, Chinese Academy of Sciences, Changchun Institute of Optics Fine Mechanics and Physics, Chinese Academy of Sciences, Changchun 130033, People's Republic of China

(Received 8 November 2012; accepted 28 December 2012; published online 17 January 2013)

Effects of magnesium on phosphorus chemical states and *p*-type conduction behavior of phosphorus-doped ZnO (ZnO:P) films were investigated by combining experiment with first-principles calculation. Photoluminescence (PL) spectra show that Mg incorporation increases the amount of V_{Zn} , which makes more $P_{Zn}-2V_{Zn}$ complex acceptor formed and background electron density decreased, leading to that MgZnO:P exhibits better *p*-type conductivity than ZnO:P. The *p*-type conductivity mainly arises from $P_{Zn}-2V_{Zn}$ complex acceptor with a shallow acceptor energy of 108 meV. X-ray photoelectron spectroscopy (XPS) spectra reveal that phosphorus has two chemical states of $P_{Zn}-2V_{Zn}$ complex and isolated P_{Zn} , with binding energy of $P_{2p3/2}$ of 132.81 and 133.87 eV, respectively. The conversion of isolated P_{Zn} to $P_{Zn}-2V_{Zn}$ complex induced by Mg incorporation is observed in XPS, in agreement with the PL results. First-principles calculations suggest that the formation energy of $nMg_{Zn}-V_{Zn}$ complex decreases with the increasing Mg content, well supporting the experiments from the PL spectra and XPS measurements. © 2013 American Institute of Physics. [<http://dx.doi.org/10.1063/1.4775840>]

I. INTRODUCTION

Although *p*-type ZnO via phosphorus doping (ZnO:P) has been obtained by various technologies,^{1–4} the reliability of *p*-type ZnO:P is still problematic. It is well known that P has amphoteric nature; it substitutes not only O site (P_O) as an acceptor, but also Zn site (P_{Zn}) as a triple donor.⁵ Some researchers attribute *p*-type conductivity to the P_O acceptor.^{6,7} However, arguments suggest that P_O should yield deep rather than shallow levels in ZnO, and thus it may not be the origin of *p*-type conductivity.^{8–10} To resolve the problem, Woo-jin Lee *et al.*¹¹ investigated *p*-type ZnO:P film by first-principle calculation and ascribed *p*-type conductivity to $P_{Zn}-2V_{Zn}$ complex acceptor. Subsequently, some groups also ascribe *p*-type conductivity observed in ZnO:P to the $P_{Zn}-2V_{Zn}$ complex acceptor.^{10,12} However, whether the $P_{Zn}-2V_{Zn}$ complex acceptor is formed still needs to be demonstrated further in experiment.

Theory calculations indicate that while Fermi energy moves towards valence-band maximum (VBM), which is a necessary condition for *p*-type conduction circumstance, the formation energy of P_{Zn} is lower than that of V_{Zn} , regardless of O-rich or Zn-rich conditions.^{11,12} This suggests that P_{Zn} is formed more easily than V_{Zn} , that is, the formation of $P_{Zn}-2V_{Zn}$ complex should be much depended on the formation of V_{Zn} . Conventionally, if the formation energy of V_{Zn} is reduced, more V_{Zn} will generate, spontaneously, more P_{Zn} may

combine with $2V_{Zn}$ to form $P_{Zn}-2V_{Zn}$ complex. That not only increases the amount of the $P_{Zn}-2V_{Zn}$ complex acceptor, but also decreases the amount of P_{Zn} donor. Obviously, decreasing formation energy of V_{Zn} may be an effective method to obtain *p*-type ZnO:P.

In the present work, we found that Mg incorporation in ZnO can decrease the formation energy of V_{Zn} , leading to that MgZnO:P film has better *p*-type conductivity than ZnO:P film. The origin of *p*-type conductivity and effect of magnesium on phosphorus chemical states were investigated by using combining experiment with first-principles calculation.

II. EXPERIMENTAL

The ZnO:P and MgZnO:P films were grown on quartz substrates by radio frequency magnetron sputtering of ZnO:P and MgZnO:P with nominal Mg content of 0.05 ceramic targets, respectively, which were fabricated by sintering high purity ZnO (99.99%), MgO (99.99%), P_2O_5 (99.998%) powders. The nominal concentration of phosphorus in the targets was 2 at. %. For comparison, undoped ZnO film was also fabricated by using high purity ZnO ceramic targets. Before deposition, the vacuum chamber was evacuated to a base pressure of 5×10^{-4} Pa and then filled with mixed gases of 99.99% pure oxygen and argon at the flux ratio of O_2/Ar of 1/3 to 1.0 Pa, which is kept during depositing process. All the films were grown for one hour, and then annealed at 800 °C for 30 min under 3×10^{-3} Pa in a tube furnace.

^{a)} Author to whom correspondence should be addressed. Electronic mail: binyao@jlu.edu.cn.

The structures of the films were characterized by x-ray diffraction (XRD) with Cu $K_{\alpha 1}$ radiation ($\lambda = 0.15406$ nm); the scan step size used is 0.02° . Electrical properties were measured in the van der Pauw configuration by a Hall Effect measurement system (LakeShore7707) at room temperature. The room temperature absorbance measurement was performed using an UV-visible-near infrared spectrophotometer (Shimadzu). The temperature-dependent photoluminescence (PL) was measured by using the UV Labran Infinity Spectrophotometer with He–Cd laser line of 325 nm as an excitation source. The composition of the films was detected by using energy dispersive x-ray spectroscopy (EDS). The chemical states of elements were characterized by x-ray photoelectron spectroscopy (XPS).

III. RESULTS AND DISCUSSION

Figure 1(a) illustrates the XRD patterns collected from the annealed undoped ZnO, ZnO:P, and MgZnO:P films. Only strong (002) and (004) diffraction peaks are observed in all films, implying that they are all of hexagonal structure with (002) preferential orientation. No MgO or P_2O_5 peaks are detected, which suggests that Mg and P atoms have doped into the lattice ZnO. The EDS measurement indicates that the composition is 54.49 at. % O, 44.59 at. % Zn, and 0.92 at. % P for ZnO:P, and 55.53 at. % O, 42.12 at. % Zn, 1.28 at. % Mg, and 1.07 at. % P for MgZnO:P, suggesting that the ZnO:P and MgZnO:P films are O-rich circumstance and have the similar contents of P. The atomic fraction of Mg is estimated to be 0.03. The lattice constant c of samples is calculated by Bragg diffraction equation, as shown in Figure 1(b). It is seen that lattice constant c of the ZnO:P decreases with respect to the undoped ZnO, suggesting that P substitutes Zn site but not O site, since the ionic radii of P^{5+} (0.031–0.034 nm) and P^{3+} (0.044–0.058 nm) are smaller than that of Zn^{2+} (0.074 nm)

TABLE I. The electrical properties of the undoped ZnO, ZnO:P, and MgZnO:P films.

Sample	Resistivity (Ω cm)	Carrier density (cm^{-3})	Mobility ($cm^2 V^{-1} s^{-1}$)	Type
ZnO	0.59	2.24×10^{18}	4.69	n
ZnO:P	16.3	Indeterminate
MgZnO:P	21.1	1.75×10^{17}	1.52	p

while the ionic radius of P^{3-} (0.18–0.212 nm) is larger than that of O^{2-} (0.138–0.14 nm). The P atom occupying Zn site (P_{Zn}) tends to contract while P atom occupying O site (P_O) tends to expand the lattice of ZnO, resulting in the decrease and increase of lattice constant c with respect to the undoped ZnO, respectively. It is well known that ionic radius of Mg^{2+} (0.057 nm) is smaller than that of Zn^{2+} (0.074 nm), the replacement of Zn^{2+} by Mg^{2+} also decreases the lattice constant c of ZnO. However, the decrease of lattice constant c induced by 0.03 at. % Mg content is calculated to be 0.0006 nm, based on our previous work.¹³ It is smaller than the difference (0.0012 nm) between the undoped ZnO and MgZnO:P, implying that P atoms similarly occupy Zn sites in the MgZnO:P.

Table I shows Hall measurement results of the undoped ZnO, ZnO:P, and MgZnO:P films. The undoped ZnO is n -type conduction, which is a common feature for an undoped ZnO due to the existence of native donor point defects (e.g., interstitial zinc, oxygen vacancies, and H impurities). However, the ZnO:P film shows indeterminate conduction type, that is, the hole density is somewhat larger than the electron density in the ZnO:P, resulting in that the Hall coefficient shows positive or negative irregularly in Hall measurement. This also implies that large numbers of acceptors and donors coexist in ZnO:P. Compared with the undoped ZnO, it is certain that the generation of holes in ZnO:P is related to P doping. More

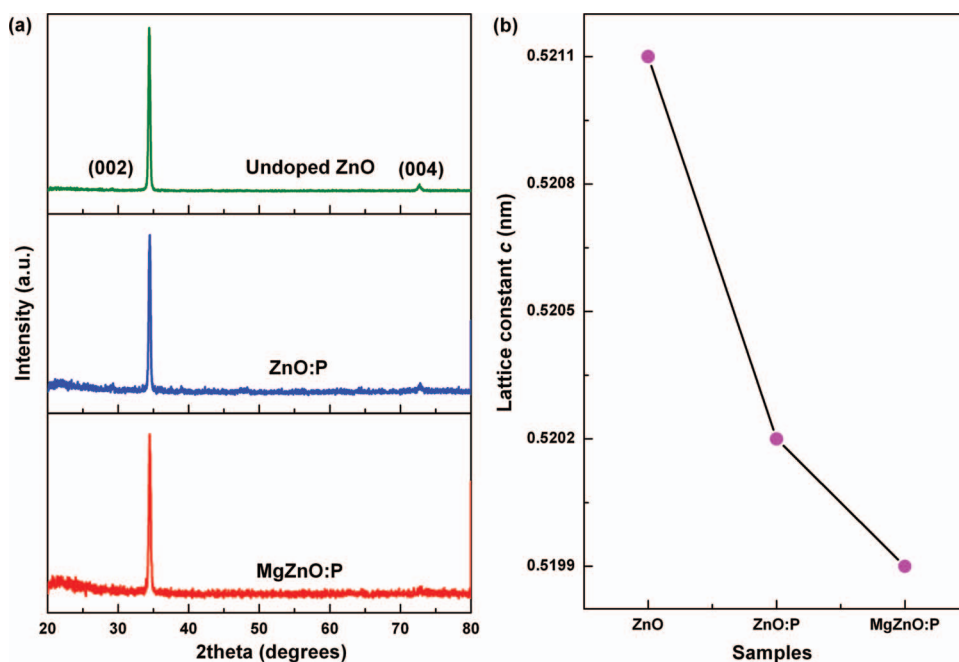


FIG. 1. (a) Typical XRD pattern of undoped ZnO, ZnO:P, and MgZnO:P films. (b) lattice constant c as a function of samples.

interesting, the MgZnO:P shows good *p*-type conductivity with a resistivity of 21.1 Ω cm, a hole concentration of $1.75 \times 10^{17} \text{ cm}^{-3}$, a mobility of $1.52 \text{ cm}^2 \text{ V}^{-1} \text{ s}^{-1}$, suggesting that Mg incorporation favors the obtaining of *p*-type conductivity. Based on our XRD results, it is deduced that hole contributor may be $\text{P}_{\text{Zn}}\text{-}2\text{V}_{\text{Zn}}$ complex in both films.^{10,12,14,15}

To well understand the role of Mg, the low-temperature PL measurements were performed for ZnO:P and MgZnO:P film at 83 K, as shown in Figures 2(a) and 2(b). For the MgZnO:P film, the spectrum consists of two emission bands at 3.356 and 2.234 eV, located at ultraviolet and visible region, respectively. In order to identify the emission band at 3.356 eV, the temperature-dependent PL is performed for MgZnO:P film, as shown in Figure 3. It can be seen that the emission band at 3.356 eV shows a continuous red-shift with the increasing temperature, and this is a typical characteristic of FA transition.

The temperature dependence of its peak position fits well in an equation for a free-neutral-acceptor (e, A^0) transition given by

$$E_{eA}(T) = E_g(T) - E_A + k_B T/2, \quad (1)$$

where $E_{eA}(T)$ is the temperature-dependent (e, A^0) transition energy, $E_g(T)$ is the band gap energy, E_A is the acceptor energy level, and k_B is the Boltzmann constant, as shown in

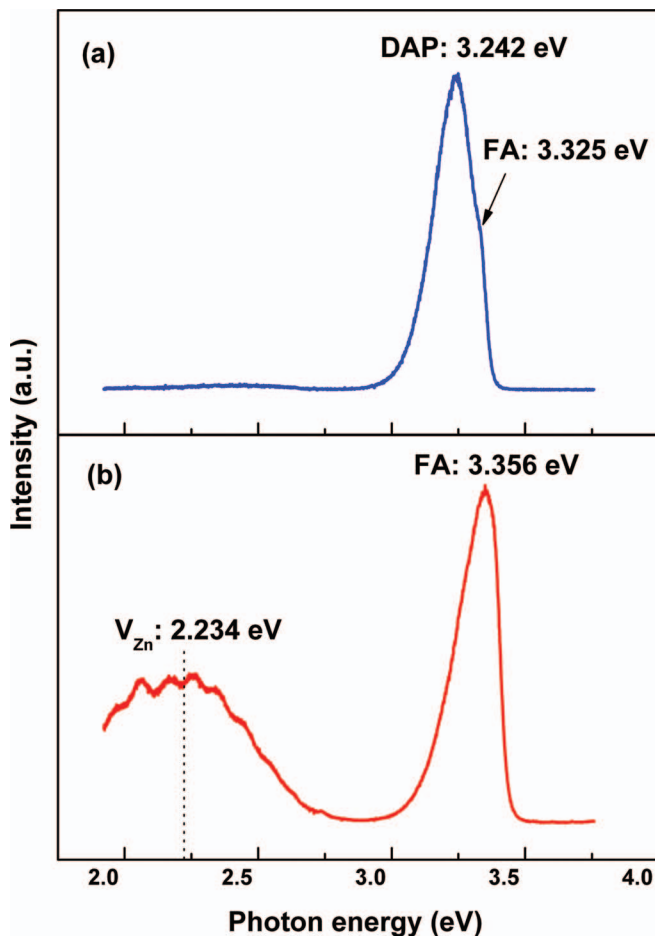


FIG. 2. Low-temperature PL spectra of (a) ZnO:P, and (b) MgZnO:P films at 83 K.

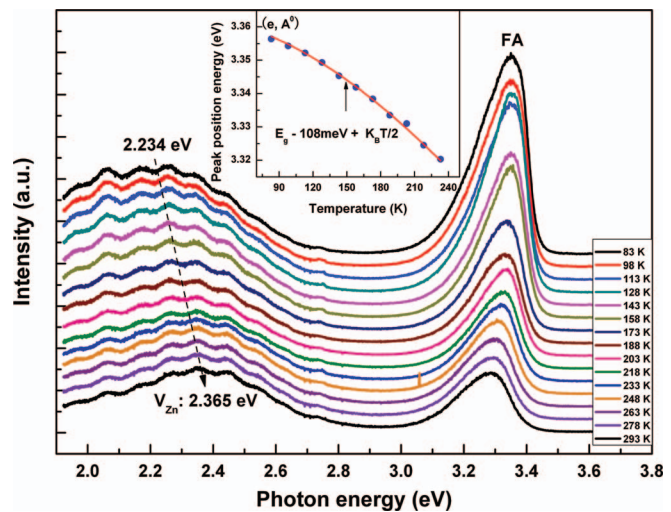


FIG. 3. Temperature-dependent PL spectra of *p*-type MgZnO:P film. The inset shows temperature-dependent peak positions of FA and the fitting curves using Eq. (1).

the inset of Figure 3. This indicates that the emission band at 3.356 eV indeed has FA nature and stems from a transition of free electron to acceptor level (FA). The large FA is due to increase of conduction-band minimum (CBM) induced by Mg incorporation. It is well known that the band gap of MgZnO increases with increasing Mg content due to the increase in the energy of the conduction-band minimum (E_c) and decrease in the energy of valence-band maximum (E_v), namely, $\Delta E_g = \Delta E_c - \Delta E_v$, $\Delta E_c > 0$ and $\Delta E_v < 0$, and the conduction-band offset is much larger than the valence-band offset ($\Delta E_c/\Delta E_v = 9/1$).¹⁶ Figure 4 shows the optical absorption spectra of ZnO:P and MgZnO:P films. It is found that band gap of the MgZnO:P is about 40 meV larger than that of ZnO:P. Calculation indicates that the band offset of CBM induced by Mg incorporation is about 36 meV, and the difference between 3.356 eV and the CBM offset is 3.320 eV, which is usually assigned to the transition of the electron from conduction band to acceptor level related to the phosphorus acceptor.^{1,17} Since the XRD measurements show

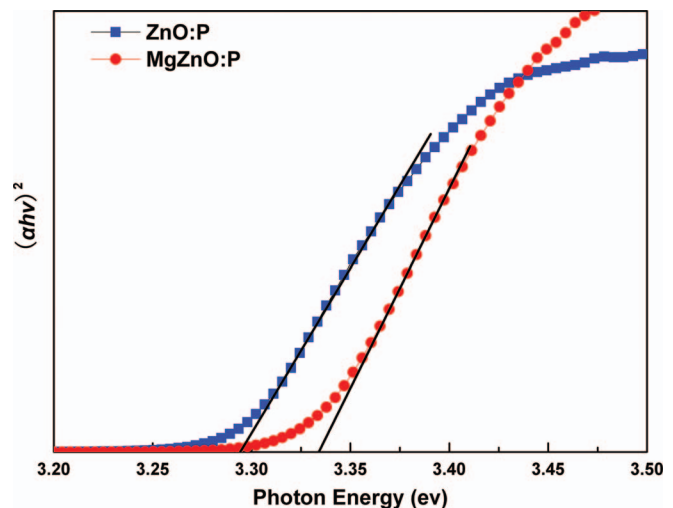


FIG. 4. Optical absorption spectra of ZnO:P and MgZnO:P films.

that P atoms mainly occupy Zn sites in MgZnO:P film, the phosphorus-related acceptor should not be P_O but $P_{Zn}-2V_{Zn}$ complex,^{10,12,14,15} of which acceptor energy is found to be 108 meV, well consistent with the previous reports.¹⁸ Previously, the FA emission peak around 3.320 eV also was observed in N-doped and As-doped ZnO.^{19,20} For the visible emission band at 2.234 eV, an obvious temperature-dependent blueshift of 131 meV from 2.234 eV at 83 K to 2.365 eV at 293 K is observed. Recently, Ahn *et al.*²¹ reported a continuous blueshift of 164 meV in visible emission from ZnO in temperature range from 10 to 300 K, which was attributed to the change of transition electrons from Zn interstitial (Zn_i) to the conduction band with increasing temperature. In the present case, the 131 meV blueshift observed from 83 K to 293 K is close to the 164 meV reported by Ahn *et al.* Therefore, we speculate that the blueshift may be due to transition electron transferring from Zn_i to conduction band as temperature increases. It is noteworthy that the emission band at 2.365 eV at 293 K is a famous green luminescence emission (GL). Recently, Ton-That *et al.*²² and Moe Borseth *et al.*²³ investigated ubiquitous GL emission in ZnO, and indicated the GL emission at 2.30 eV in O-rich ZnO and at 2.52 eV in Zn-rich ZnO stems from the transition of free electron to V_{Zn} and V_O , respectively. First-principles calculations also demonstrated that the transition from conduction-band electron to the $1-/2-$ acceptor level of V_{Zn} could give rise to PL emission around 2.30 eV.²⁴⁻²⁶ It has been suggested from EDS measurement that the MgZnO:P film is O-rich circumstance. The difference between 2.365 eV and the CBM offset induced by Mg incorporation is 2.329 eV, which basically accords with the reported 2.30 eV by Ton-That *et al.*²² and Moe Borseth *et al.*²³ Therefore, the emission band at 2.365 eV is ascribed to the transition of free electron to V_{Zn} , implying that large numbers of V_{Zn} exist in MgZnO:P film. Moreover, one can see that the visible emission band located at 2.234 eV possesses an evident vibrational structure with interval energy of about 100 meV. The vibrational structure likely comes from the interference between the upper and lower interfaces of the MgZnO:P film,^{27,28} and hence their energy position does not change with the measurement temperature. The appearance of such interference peaks indicates that the film is very smooth.

For the ZnO:P film, the spectrum also reveals two emission peaks at 3.325 and 3.242 eV. The acromino-peak at 3.325 eV is attributed to the transition of free electron to $P_{Zn}-2V_{Zn}$ complex acceptor (FA). It has been suggested from Table I that larger numbers of acceptors and donors coexist in the ZnO:P, therefore, the dominant emission peak at 3.242 eV can be tentatively assigned to a recombination of donor-acceptor pair (DAP). To support the assignment, the temperature-dependent PL was performed for the ZnO:P, as shown in Figure 5. It is seen that the emission peak at 3.242 eV shows distinctly blueshift first, and then gradually merges into the FA due to thermal ionization of donors with the increasing temperature, and this is a typical characteristic of DAP transition.^{29,30} Obviously, the emission peak at 3.242 eV indeed arises from the DAP transition. Furthermore, the visible emission of ZnO:P is extremely weak, implying that the ZnO:P film has little deep level defects. Hence, the acceptor involved in DAP transition may be $P_{Zn}-2V_{Zn}$ complex.

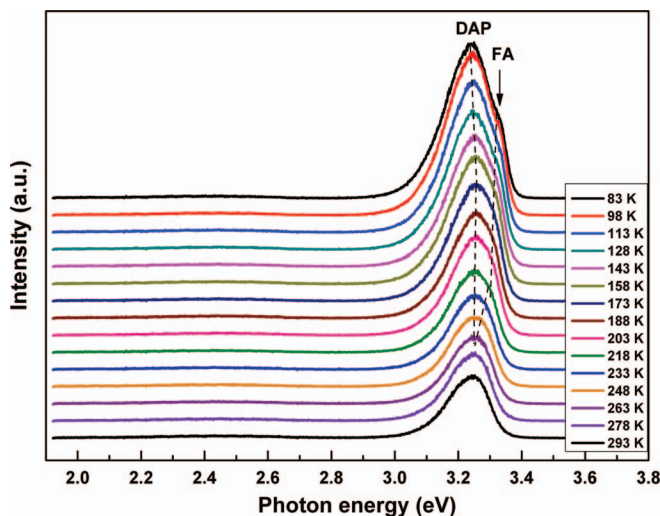


FIG. 5. Temperature-dependent PL spectra of ZnO:P film.

Actually, Hwang *et al.*¹⁷ also observed the peak in ZnO:P film and attributed it to the DAP transition related to phosphorus acceptor. Herein, it should be noted that the peak related to V_{Zn} is not observed in ZnO:P, suggesting that formation of the $P_{Zn}-2V_{Zn}$ complex is greatly restrained by the shortage of the V_{Zn} . Although the $P_{Zn}-2V_{Zn}$ complex acceptor has been formed in ZnO:P, it is insufficient and cannot completely compensate donors, therefore, the conduction type of ZnO:P is indeterminate shown in Hall measurement and the dominant DAP transition reveals in 83 K PL spectrum. However, for MgZnO:P film, the observation of the peak related to V_{Zn} indicates there are still excess V_{Zn} except the V_{Zn} combined with P_{Zn} to form $P_{Zn}-2V_{Zn}$ complex in the MgZnO:P. The abundant V_{Zn} not only promotes the formation of $P_{Zn}-2V_{Zn}$ complex, but also can compensate some native donors. Obviously, Mg incorporation increases the amount of V_{Zn} , which makes more $P_{Zn}-2V_{Zn}$ complex acceptor formed and background electron density decreased, leading to good p -type conductivity in MgZnO:P. Moreover, it is generally known that V_{Zn} has deeper acceptor level than the $P_{Zn}-2V_{Zn}$ complex.^{31,32} The domination of FA transition suggests $P_{Zn}-2V_{Zn}$ complex is mainly responsible for p -type conductivity.

To further support the PL results, XPS measurement was performed for the ZnO:P and MgZnO:P films, as shown in Figures 6(a) and 6(b), respectively. The XPS peak of $P_{2p_{3/2}}$ can be well fitted by two sub-peaks located at 132.88 and 133.85 eV in ZnO:P, implying that the P has two chemical states. Wang *et al.*³³ reported that the binding energy (BE) of $P_{2p_{3/2}}$ in P-Zn bond is about 129 eV, which are far away the BE value shown in Figure 6(a), implying that the P atom does not occupy O site. Onyiriuka³⁴ investigated XPS of zinc phosphate glass composed mainly of ZnO and P_2O_5 and found that the BE of $P_{2p_{3/2}}$ in P-O-P and P-O-Zn bond is between 133.3 and 133.8 eV, which is closed to the BE of $P_{2p_{3/2}}$ of ZnO: P, therefore, the two $P_{2p_{3/2}}$ sub-peaks located at 132.88 and 133.85 eV are ascribed to P_{Zn} , implying that P atoms occupy Zn sites in ZnO:P film, consistent with the XRD results. Based on the XRD and PL above, it is concluded that the isolated P_{Zn} and $P_{Zn}-2V_{Zn}$ complex are main existence form of

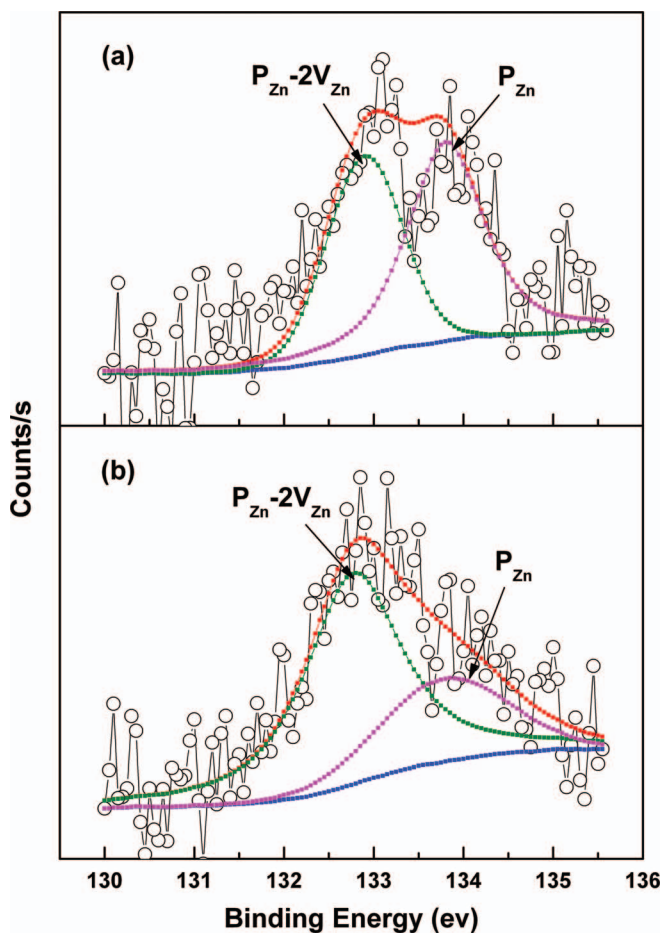


FIG. 6. XPS spectra and fitting curves of (a) ZnO:P, and (b) MgZnO:P films.

P_{Zn} , therefore, the two $P_{2p_{3/2}}$ sub-peaks should stem from isolated P_{Zn} and $P_{Zn}-2V_{Zn}$ complex. Theory calculations^{11,12} indicate that the formation energy of P_{Zn}^{3+} is lower than that of P_{Zn}^{2+} , P_{Zn}^{1+} , and P_{Zn} , respectively, implying that P_{Zn} more easily loses three electrons to become positive trivalent P_{Zn}^{3+} . If P_{Zn} transfer the electrons to conduction band, it will become isolated P_{Zn}^{3+} , but if P_{Zn} is neighboring with two V_{Zn} defects, a charge transfer of three electrons from P_{Zn} to V_{Zn} happens, and the strong Coulomb interactions between the oppositely charged P_{Zn}^{3+} and V_{Zn}^{2-} defects will drive the P_{Zn}^{3+} and V_{Zn}^{2-} to form the $P_{Zn}-2V_{Zn}$ complex acceptor. Simultaneously, the $P_{Zn}-2V_{Zn}$ complex can obtain an electron from valence band to become $(P_{Zn}-2V_{Zn})^-$ complex. Obviously, P_{Zn}^{3+} in $(P_{Zn}-2V_{Zn})^-$ complex has four electrons more than isolated P_{Zn}^{3+} , and the four electrons have an additional effect of screening the P_{Zn}^{3+} , which reduces the BE of $P_{2p_{3/2}}$ of $(P_{Zn}-2V_{Zn})^-$ complex, implying that the BE of $P_{2p_{3/2}}$ of $(P_{Zn}-2V_{Zn})^-$ complex is smaller than that of isolated P_{Zn}^{3+} . Therefore, the two peaks at 132.88 and 133.85 eV is reasonably assigned to the $P_{2p_{3/2}}$ of $(P_{Zn}-2V_{Zn})^-$ complex and isolated P_{Zn}^{3+} , respectively.

For the MgZnO:P, the XPS spectrum also reveals two sub- $P_{2p_{3/2}}$ peaks, located at 132.81 and 133.87 eV, respectively, which are almost the same as the ZnO:P. This is because: (i) both P and Mg substitute Zn sites and cannot become nearest neighboring each other; (ii) Mg and Zn have the same valence state, when Mg substitutes Zn site, it cannot

change electric field around it, implying that Mg incorporation do not basically influence the BE of $P_{2p_{3/2}}$. Similar to the ZnO:P, the two sub- $P_{2p_{3/2}}$ peaks at 132.81 and 133.87 eV are also attributed to $(P_{Zn}-2V_{Zn})^-$ and isolated P_{Zn}^{3+} , respectively. According to XPS theory, the peak area (intensity) of $P_{Zn}-2V_{Zn}$ complex and isolated P_{Zn} is proportional to the content of $P_{Zn}-2V_{Zn}$ complex and P_{Zn} .^{35,36} The peak area ratio of $(P_{Zn}-2V_{Zn})^-$ to P_{Zn}^{3+} is calculated to be 0.77 for the ZnO:P and 2.52 for the MgZnO:P, respectively. It is evident that the ratio of $P_{Zn}-2V_{Zn}$ to P_{Zn} in MgZnO:P is larger than that in ZnO:P. This indicates that part of P_{Zn} donors convert to $P_{Zn}-2V_{Zn}$ complex acceptors as Mg incorporates in ZnO:P. This not only increases the $P_{Zn}-2V_{Zn}$ complex acceptors, but also decreases P_{Zn} donors, consequently, leading to that MgZnO:P has better p -type conductivity than ZnO:P, well supporting the PL results above.

To better understand the increase of V_{Zn} as Mg alloyed into ZnO, we carry out first-principles calculations using the Vienna Ab Initio Simulation Package (VASP) code with the projector augmented wave (PAW) potentials and generalized gradient approximation (GGA).^{37,38} In all the calculations, we construct 72-atom $3 \times 3 \times 2$ supercells with the wurtzite structures. For the Brillouin zone integration, a $2 \times 2 \times 2$ k-point mesh is used. All the atoms are allowed to relax until the Hellmann–Feynman forces become less than 0.01 eV/Å. The cutoff energy for the plane-wave basis set is 400 eV. To simulate the Mg-alloyed ZnO structure with V_{Zn} , a Zn atom is removed and the nearest neighbor (NN) six Zn atoms are substituted by Mg atoms (Mg_{Zn}) in the lattice for simulating $nMg_{Zn}-V_{Zn}$ complex. The formation energy of the $nMg_{Zn}-V_{Zn}$ complex with electric neutrality can be expressed as

$$\Delta H_f(nMg_{Zn} - V_{Zn}) = E_{tot}(nMg_{Zn} - V_{Zn}) - E_{tot}(ZnO) + (n+1)\mu_{Zn} - n\mu_{Mg}, \quad (2)$$

where $E_{tot}(nMg_{Zn}-V_{Zn})$ is the total energy of the supercell with the $nMg_{Zn}-V_{Zn}$ complex; $E_{tot}(ZnO)$ is the total energy of the perfect ZnO supercell; and n indicates the number of Mg atoms in the supercell. μ_{Zn} and μ_{Mg} are chemical potentials of Mg and Zn referenced to the elemental solid energy. To keep ZnO stable and avoid the phase separation, it is required that $\mu_{Zn} + \mu_O = H_f(ZnO)$, for example, the formation of MgO, μ_O is limited by $\mu_{Mg} + \mu_O \leq H_f(MgO)$, where $H_f(ZnO)$ and $H_f(MgO)$ are the formation energy of ZnO and MgO. In our calculation, the $H_f(ZnO)$ and $H_f(MgO)$ are -6.0 eV and -3.4 eV, respectively, which are in good agreement with the experimental values.³⁹

Figure 7 shows the formation energy of $nMg_{Zn}-V_{Zn}$ complex as a function of Mg content under the metal-rich and O-rich limit. It is found that the formation energy of $nMg_{Zn}-V_{Zn}$ complex decreases with the increasing Mg content, indicating that the formation of V_{Zn} is favored at the higher Mg content, which is in agreement with the previous work by Li *et al.*⁴⁰ The calculated results well support the experiments from the PL spectra and XPS measurements. Moreover, it is noted that, at low Mg content, the formation energy of $nMg_{Zn}-V_{Zn}$ complex under O-rich limit is less than one under O-poor limit, which is understandable result in experiment. The formation of cation vacancy (V_{Zn}) is favored under O-rich condition.

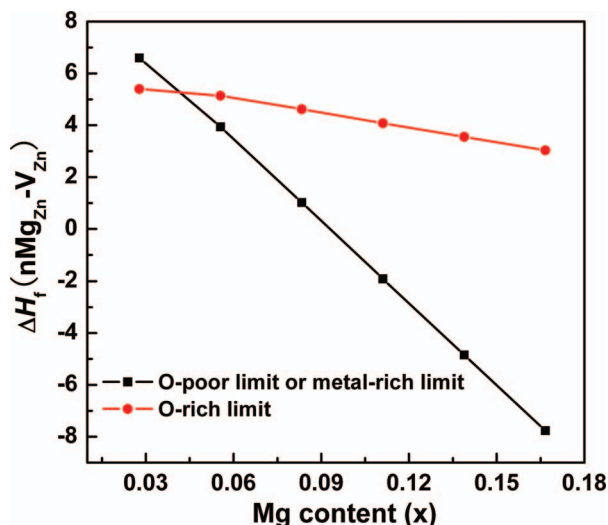


FIG. 7. Formation energy of $n\text{MgZn-V}_{\text{Zn}}$ complex as a function of Mg content under metal-rich and O-rich limit.

The formation energy of $n\text{MgZn-V}_{\text{Zn}}$ complex under O-poor limit rapidly decreases with the increase of Mg content. As Mg content is above 0.04, the formation energy of $n\text{MgZn-V}_{\text{Zn}}$ complex under O-rich limit is larger than one under O-poor limit. Under O-poor condition, there is a competition between Zn and Mg for bonding with oxygen. In this case, Mg is favored due to stronger chemical reactivity of Mg than Zn. Therefore, at higher Mg content, $n\text{MgZn-V}_{\text{Zn}}$ complex has a lower formation energy under O-poor limit than under O-rich.

IV. CONCLUSION

In summary, the undoped ZnO, ZnO:P, and MgZnO:P films are prepared on quartz substrates by radio frequency magnetron sputtering. Our experimental data combined with the first-principles calculations suggest that incorporation of Mg increases the amount of the V_{Zn} , which not only converts P chemical states from isolated P_{Zn} donor to $\text{P}_{\text{Zn}}-2V_{\text{Zn}}$ complex acceptor, but also decreases background electron concentration, leading to that the MgZnO:P has better p -type conductivity than ZnO:P. The hole contributor is mainly $\text{P}_{\text{Zn}}-2V_{\text{Zn}}$ complex acceptor, the ionized energy of which is estimated to be 108 meV. These results indicate that Mg incorporation may be a promising method for realizing reliable p -type ZnO:P.

ACKNOWLEDGMENTS

This work was supported by the National Natural Science Foundation of China under Grant Nos. 10874178, 11074093, 61205038 and 11274135, Natural Science Foundation of Jilin province under grant No. 201115013, and National Found for Fostering Talents of Basic Science under grant No. J1103202.

¹D. K. Hwang, H. S. Kim, J. H. Lim, J. Y. Oh, J. H. Yang, S. J. Park, K. K. Kim, D. C. Look, and Y. S. Park, *Appl. Phys. Lett.* **86**, 151917 (2005).

²F. X. Xiu, Z. Yang, L. J. Mandalapu, and J. L. Liu, *Appl. Phys. Lett.* **88**, 152116 (2006).

- ³J. D. Ye, S. L. Gu, S. M. Zhu, S. M. Liu, Y. D. Zheng, R. Zhang, Y. Shi, Q. Chen, H. Q. Yu, and Y. D. Ye, *Appl. Phys. Lett.* **88**, 101905 (2006).
- ⁴H. S. Kim, F. Lugo, S. J. Pearton, D. P. Norton, Y. L. Wang, and F. Ren, *Appl. Phys. Lett.* **92**, 112108 (2008).
- ⁵A. Allenic, W. Guo, Y. B. Chen, M. B. Katz, G. Y. Zhao, Y. Che, Z. D. Hu, B. Liu, S. B. Zhang, and X. Q. Pan, *Adv. Mater.* **19**, 3333 (2007).
- ⁶M. S. Oh, D. K. Hwang, Y. S. Choi, J. W. Kang, S. J. Park, C. S. Hwang, and K. I. Cho, *Appl. Phys. Lett.* **93**, 111905 (2008).
- ⁷D. K. Hwang, M. S. Oh, J. H. Lim, C. G. Kang, and S. J. Park, *Appl. Phys. Lett.* **90**, 021106 (2007).
- ⁸Y. R. Ryu, T. S. Lee, and H. W. White, *Appl. Phys. Lett.* **83**, 87 (2003).
- ⁹D. C. Look and B. Claflin, *Phys. Status Solidi B* **241**, 624 (2004).
- ¹⁰H. S. Kim, S. J. Pearton, D. P. Norton, and F. Ren, *J. Appl. Phys.* **102**, 104904 (2007).
- ¹¹W. J. Lee, J. Kang, and K. J. Chang, *Phys. Rev. B* **73**, 024117 (2006).
- ¹²P. Li, S. H. Deng, and J. Huang, *Appl. Phys. Lett.* **99**, 111902 (2011).
- ¹³S. C. Su, Y. M. Lu, Z. Z. Zhang, B. H. Li, D. Z. Shen, B. Yao, J. Y. Zhang, D. X. Zhao, and X. W. Fan, *Appl. Surf. Sci.* **254**, 4886–4890 (2008).
- ¹⁴S. Limpijumnong, S. B. Zhang, S. H. Wei, and C. H. Park, *Phys. Rev. Lett.* **92**, 155504 (2004).
- ¹⁵H. F. Liu and S. J. Chua, *Appl. Phys. Lett.* **96**, 091902 (2010).
- ¹⁶Y. F. Li, B. Yao, Y. M. Lu, Z. P. Wei, Y. Q. Gai, C. J. Zheng, Z. Z. Zhang, B. H. Li, D. Z. Shen, X. W. Fan, and Z. K. Tang, *Appl. Phys. Lett.* **91**, 232115 (2007).
- ¹⁷D. K. Hwang, M. S. Oh, Y. S. Chi, and S. J. Park, *Appl. Phys. Lett.* **92**, 161109 (2008).
- ¹⁸A. Allenic, W. Guo, Y. B. Chen, Y. Che, Z. D. Hu, B. Liu, and X. Q. Pan, *J. Phys. D* **41**, 025103 (2008).
- ¹⁹M. Ding, D. X. Zhao, B. Yao, B. H. Li, Z. Z. Zhang, and S. D. Zhen, *Appl. Phys. Lett.* **98**, 062102 (2011).
- ²⁰W. Lee, M. C. Jeong, and J. M. Myoung, *Appl. Phys. Lett.* **85**, 6167 (2004).
- ²¹C. H. Ahn, Y. Y. Kim, D. C. Kim, S. K. Mohanta, and H. K. Cho, *J. Appl. Phys.* **105**, 013502 (2009).
- ²²C. Ton-That, L. Weston, and M. R. Phillips, *Phys. Rev. B* **86**, 115205 (2012).
- ²³T. Moe Borseth, B. G. Svensson, A. Y. Kuznetsov, P. Klason, Q. X. Zhao, and M. Willander, *Appl. Phys. Lett.* **89**, 262112 (2006).
- ²⁴A. F. Kohan, G. Ceder, D. Morgan, and C. G. Van de Walle, *Phys. Rev. B* **61**, 15019 (2000).
- ²⁵A. Janotti and C. G. Van de Walle, *Phys. Rev. B* **76**, 165202 (2007).
- ²⁶M. G. Wardle, J. P. Goss, and P. R. Briddon, *Phys. Rev. B* **72**, 155108 (2005).
- ²⁷H. Zhu, C. X. Shan, B. H. Li, J. Y. Zhang, B. Yao, Z. Z. Zhang, D. X. Zhao, D. Z. Shen, and X. W. Fan, *J. Phys. Chem. C* **113**, 2980–2982 (2009).
- ²⁸H. Tampo, H. Shibata, K. Maejima, A. Yamada, K. Matsubara, P. Fons, S. Niki, T. Tainaka, Y. Chiba, and H. Kanie, *Appl. Phys. Lett.* **91**, 261907 (2007).
- ²⁹B. K. Meyer, H. Alves, D. M. Hofmann, W. Kriegseis, D. Forster, F. Bertram, J. Christen, A. Hoffmann, M. Strabburg, M. Dworzak, U. Haboeck, and A. V. Rodina, *Phys. Status Solidi B* **241**, 231 (2004).
- ³⁰K. Tamura, T. Makino, A. Tsukazaki, M. Sumiya, S. Fuke, T. Furumochi, M. Lippmaa, C. H. Chia, Y. Segwa, H. Koinuma, and M. Kawasaki, *Solid State Commun.* **127**, 265 (2003).
- ³¹S. H. Jeong, B. S. Kim, and B. T. Lee, *Appl. Phys. Lett.* **82**, 2625 (2003).
- ³²Y. R. Sui, B. Yao, Z. Hua, G. Z. Xing, X. M. Huang, T. Yang, L. L. Gao, T. Zhao, H. L. Pan, H. Zhu, W. W. Liu, and T. Wu, *J. Phys. D* **42**, 065101 (2009).
- ³³Y. P. Wang, J. Q. Zhou, Q. Lu, L. L. Liu, X. Zhang, and X. J. Wu, *J. Appl. Phys.* **49**, 041103 (2010).
- ³⁴E. C. Onyiriuka, *J. Non-Cryst. Solids* **163**, 268 (1993).
- ³⁵H. Yuan, B. Luo, S. A. Campbell, and W. L. Gladfelter, *Electrochem. Solid-State Lett.* **14**(5), H181–H183 (2011).
- ³⁶L. L. Gao, B. Yao, B. Liu, L. Liu, T. Yang, B. B. Liu, and D. Z. Shen, *J. Chem. Phys.* **133**, 204501 (2010).
- ³⁷J. P. Perdew, K. Burke, and M. Ernzerhof, *Phys. Rev. Lett.* **77**, 3865 (1996).
- ³⁸P. E. Blöchl, *Phys. Rev. B* **50**, 17953 (1994).
- ³⁹W. R. Veazey and C. D. Hodgman, *Handbook of Chemistry and Physics*, 84th ed. (CRC, 1914).
- ⁴⁰Y. F. Li, R. Deng, B. Yao, G. Z. Xing, D. D. Wang, and T. Wu, *Appl. Phys. Lett.* **97**, 102506 (2010).